CONDITIONS OF PARAMETRIC ROLLING

Vladimir Shigunov, Ould El Moctar, Helge Rathje

Germanischer Lloyd AG, Hamburg, vladimir.shigunov@gl-group.com

ABSTRACT

The paper considers conditions of parametric rolling with particular attention to the influence of *GM* and forward speed. Numerical and experimental results, illustrating the theoretical considerations, are shown for two container ships in regular and irregular waves.

Keywords: *parametric rolling, synchronous rolling, numerical simulation*

1. INTRODUCTION

Present IMO efforts towards the new generation performance-based intact stability criteria require better understanding of the physical problems addressed, and their better handling in simulations and experiments. For container ships, the following dynamic stability problems are most relevant: synchronous rolling, principal parametric resonance and fundamental parametric resonance. Principal or low-cycle parametric rolling was initially of practical concern mostly for smaller ships with marginal stability in following seas, in relation to capsizing (see Kempf, 1938, Graff & Heckscher, 1941, Kerwin, 1955, Paulling, 1961). The early studies had revealed that for principal parametric resonance, the natural roll period should be close to twice the wave encounter period, and wave length should be close to the ship length. As a result of these studies, IMO released operational guidelines for ship masters, indicating dangerous situations in following and quartering seas (MSC/Circ.707, 1995), where wave directions up to 45° off-stern and wave encounter periods close to half the natural roll period were identified as dangerous for parametric rolling.

Due to several accidents with ships operating in head seas (France et al., 2003, Hua et al., 2006), attention to parametric roll also in head waves has increased. Model tests and full-scale observations have shown that principal parametric resonance can occur not only in long-crested longitudinal (head or following) waves, but also at slightly oblique heading angles, with and without directional wave spreading (see e.g. Hashimoto et al., 2006).

The present paper shows that parametric roll can be more dangerous in oblique waves for certain load cases and speeds. Several container ships were studied, ranging from a feeder ship to a 13000 TEU-container carrier, each for a broad range of loading conditions, in order to verify the conclusions. Detailed resulzs can be found in SLF 51/INF.3 (2008); this paper shows examples for two container ships (ships B and C), with $L_{pp} = 319$ and 317 m and $B_{wl} = 43.2$ and 42.8 m, respectively, for the range of GM from 0.88 to 7.5 m.

2. NUMERICAL TOOLS

Many numerical methods are used for the simulation of parametrically excited roll mo-

tion, ranging from the uncoupled non-linear roll equation (Francescutto & Bulian, 2002, Umeda et al., 2003, Bulian et al., 2003) to models accounting for the influence of other degrees of freedom on roll (Söding, 1982, DeKat & Paulling, 1989, Belenky et al., 2003, Neves & Rodríguez, 2006, Spanos & Papanikolaou, 2006).

Early models, based on uncoupled roll motion and static equilibrium for vertical motions (Paulling, 1961), were sufficient for the following seas situations; studies of parametric roll in head seas have shown that the nonlinear influence of the vertical motions on roll (through *GM* variations and inertia terms) is also important for parametric resonance (see discussion in Neves & Rodríguez, 2006, Ahmed et al., 2006, Spanos & Papanikolaou, 2006), together with the nonlinear variation of the restoring moment. On the other hand, linear radiation and diffraction for all d.o.f. is usually assumed sufficient (Neves & Rodríguez, 2006, Spanos & Papanikolaou, 2006); it is unclear yet how important is the nonlinear excitation due to waves and the feedback from roll to the vertical motions; in some situations, steady ship wave system can also be important.

Two nonlinear time-domain ship motion simulation methods were used: *rolls* and *GL SIMBEL*. The method *rolls* (roll simulation) was established by Söding (1982) and further developed by Kröger (1987), for external loads and ship motions, and Petey (1986), for flow in tanks and damaged compartments. The method was designed to simulate accurately the roll motion, whereas other motions are treated in order to account for their influence on roll. The degrees of freedom are separated into two groups: those for which hydrodynamic effects are usually relatively small, but forces and moments depend strongly nonlinearly on wave and motion amplitudes (roll and surge) and those for which nonlinearity is less important (heave, pitch, sway and yaw).

For these different groups of motions, different numerical methods are applied: heave, pitch, sway and yaw are computed in the frequency domain using a linear method; the motion history in an irregular seaway is found for them as a superposition of reactions to harmonic waves. For surge and roll, the relatively small hydrodynamic effects are simplified, while the nonlinear hydrostatic and Froude-Krylov forces are treated accurately, taking account of the instantaneous ship attitude and wave. The numerical method uses the concept of Grim (1961) equivalent wave in the form proposed by Söding (1982). The parameters of the equivalent wave are computed using transfer functions between them and the regular wave components constituting the seaway; these transfer functions are calculated before simulations using the least-square method. Nonlinear surge force is calculated following the idea of Blume (1976), who demonstrated that the Froude-Krylov force is almost exclusively responsible for the surge motion for such slender bodies as container ships.

The advantage of the *rolls* approach as compared to fully non-linear formulations is large computational speed (about $2 \cdot 10^4$ and 10^3 times quicker than real time for regular and irregular waves, respectively), still retaining coupling between the all 6 d.o.f., important for large-amplitude roll motions.

Recent applications of *rolls* to practical problems can be found in Krüger & Kluwe (2006) and SLF 51/INF.3 (2008).

The method *GL SIMBEL* is based on the work of Söding (1982), Böttcher (1986) and Pereira (1988). All 6 degrees of rigid-body ship motions are simulated using nonlinear motion equations. The Froude-Krylov forces and moments are found by integration of the pressure field over the instantaneous wetted ship surface. Radiation and diffraction forces are determined by a nonlinear strip method, depending on the relative motions between the sections and surrounding water, together with their time derivatives up to a sufficiently high order to model the previous history (i.e. the frequency dependence of the added mass, damping and wave excitation forces).

Both methods *rolls* and *GL SIMBEL* use a prescribed roll damping moment, composed of linear, quadratic and cubic contributions. The coefficients of these contributions were found from model tests using two methods: free roll decay tests and stationary roll motion excited by a rotating eccentric (Blume, 1979); roll damping due to wave radiation was subtracted from the measured damping. Alternatively, empirical correlations or RANSE simulations (e.g. Salui et al., 2004) can be used.

Hennig et al. (2006) carried out validation of *rolls* in customised irregular wave trains. Brunswig et al. (2006) showed comparison of *rolls* results with measurements in regular head and following waves. In 2007, GL has carried out two series of model tests for ship B for validation of *rolls* and *GL SIMBEL*: tests at MARIN regarding parametric and synchronous roll in regular waves in a wide range of loading conditions, wave directions and periods and model speeds, and tests at HSVA concerning the influence of the forward speed on parametric roll in regular and irregular head waves. A detailed description of these two series of tests and validation results will be published elsewhere; some results are shown in SLF 50/INF.2 (2007) and SLF 51/INF.3 (2008), together with a more detailed description of the numerical methods.

3. CONDITIONS OF PARAMETRIC ROLLING

First, find the combinations of wave frequency ω and wave direction μ leading to a given encounter frequency ω_e, equal to the natural roll frequency ω_φ for synchronous rolling and fundamental parametric resonance or $2\omega_\varphi$ for principal parametric resonance. For the ship in head waves or in long following overtaking waves, we have

$$\omega = \left(g - \sqrt{g^2 - 4gv\omega_e \cos\mu} \right) \Big/ \left(2v\cos\mu \right), \quad (1)$$

with the limit $\omega \to \omega_e$ for $\mu \to \pm\pi/2$. If the ship is overtaken by shorter following waves,

$$\omega = \left(g + \sqrt{g^2 - 4gv\omega_e \cos\mu} \right) \Big/ \left(2v\cos\mu \right). \quad (2)$$

For following waves in cases (1) and (2), the limitation applies $\omega_e < g/(4v\cos\mu)$, leading to the limitation on the wave encounter angle $\cos^{-1}\left[g/(4v\omega_e) \right] < \mu < \pi/2$ for speeds larger than $g/(4\omega_e)$. If the ship overtakes short following waves,

$$\omega = \left(g + \sqrt{g^2 + 4gv\omega_e \cos\mu} \right) \Big/ \left(2v\cos\mu \right). \quad (3)$$

The lines for which these conditions are satisfied (resonance lines) are shown in axes wave period *T* (radial coordinate) – wave direction μ (circumferential) in Figure 1 for $\omega_e = 2\omega_\varphi$ (top) and ω_φ (bottom), for ship B with *GM*=3.8 m, for seven uniformly distributed speeds from 0 to 23.3 knots. Two lines are shown for each speed: solid line corresponding to bow waves and overtaking stern waves, i.e. conditions (1) and (2), and dashed one corresponding to stern waves overtaken by the ship, condition (3). The latter condition leads for the relatively large and slow ships to very short waves, which do not represent a danger.

For conditions (1) and (2), pure following waves cannot lead to the encounter frequency $\omega_e = 2\omega_\varphi$ for the speeds larger than $g/(8\omega_\varphi)$, and the suitable areas for resonance shift towards stern-quartering waves. The larger the ship speed, the more the resonance line is shifted towards beam waves, with the minimum wave encounter angle defined as $\cos^{-1}\left[g/(4v\omega_\varphi) \right]$.

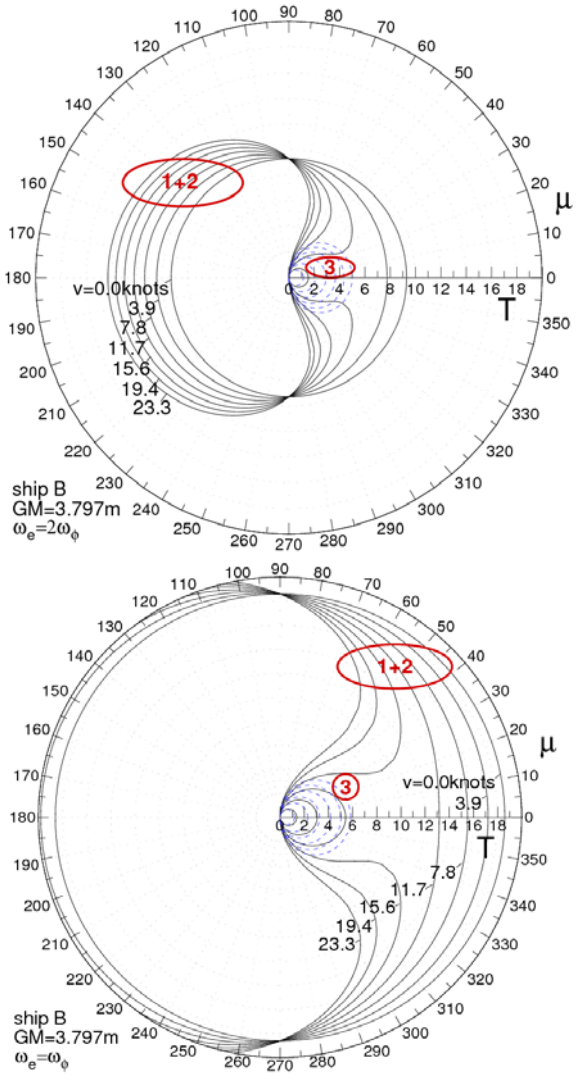

Figure 1. Resonance conditions for principal parametric rolling (top) and synchronous rolling and fundamental resonance (bottom): solid lines "1+2" correspond to conditions (1) and 2, and dashed lines "3" to condition (3).

The second condition for parametric resonance is related to the fact that maximum changes of righting levers happen if the midship is located near a wave crest when bow and stern are located in neighbour troughs and vice versa. In longitudinally running waves, this means that the wave length should be close to the ship length. Depending on the hull form and the strength of the coupling of roll with pitch and heave motions, this condition usually leads to a range of the critical wave lengths, from about 0.5 to 2 ship lengths (in longitudinally running waves).

In oblique waves, bow and stern lie in the neighbour wave troughs (or stay on the neighbour wave crests) if the wave length is $\lambda_w = L_{pp} \cos\mu$, or for a range of wave lengths,

$$\frac{L_{pp}}{2}\cos\mu < \lambda_w < 2L_{pp}\cos\mu . \qquad (4)$$

This condition is satisfied in two domains on the polar plot, corresponding to bow and stern waves (Figure 2). Combining the two conditions of principal parametric resonance (Figure 3), the areas of possible principal parametric resonance can be identified as the parts of the resonance lines within the suitable wave length areas (thick lines). For this load case, parametric rolling in stern waves appears possible only for stern-quartering directions.

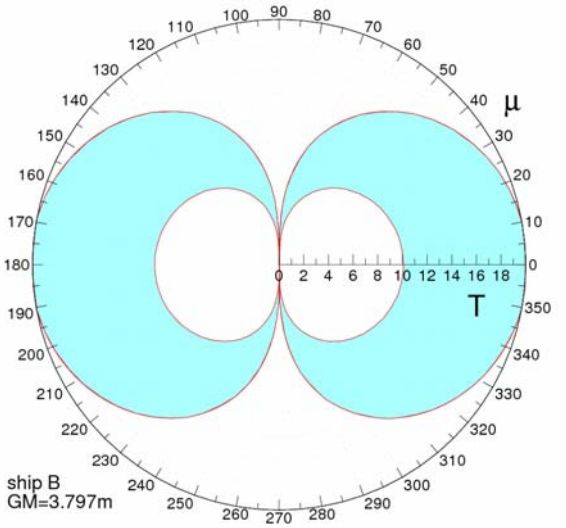

Figure 2. Wave periods and directions corresponding to the suitable wave lengths (4).

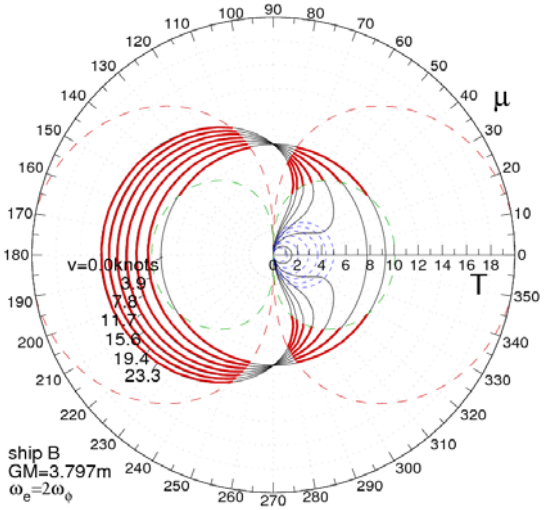

Figure 3. Combined resonance and wave length conditions for ship B with

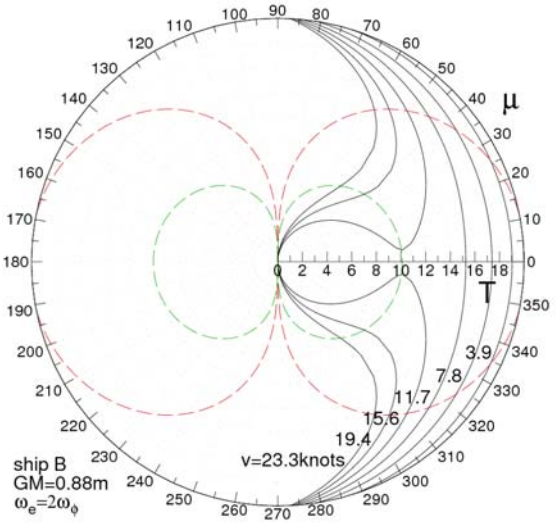

Figure 4. Critical areas for *GM*=0.88 m

GM=3.797 m.

4. INFLUENCE OF *GM*

Consider for ship B the loading cases with *GM*=0.88, 1.26, 3.797 and 7.5 m. Figure 4 shows the critical areas for *GM*=0.88 m. Only the resonance lines corresponding to $T_e = T_\varphi / 2$ are plotted, as the condition $T_e = T_\varphi$ leads for this case to very large wave periods, which are not relevant in real seaways. Resonance lines corresponding to waves overtaken by the ship are also not shown, as such waves are too short to represent any danger. The dashed lines correspond to the minimum and maximum critical wave lengths (4). Parametric roll appears possible in following waves for speeds up to about half design speed; for larger speeds, resonance shifts towards stern-quartering waves.

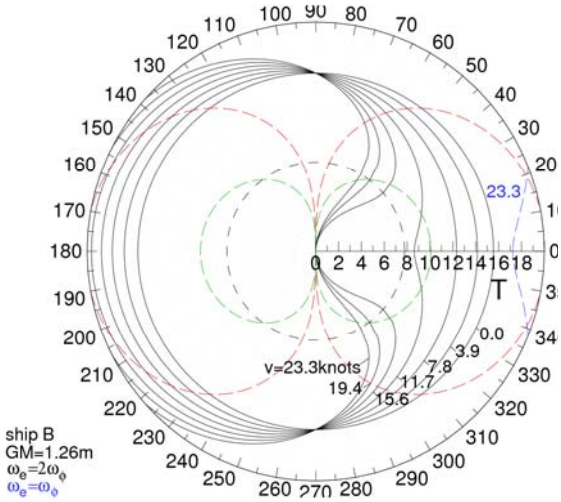

Figure 5. Critical areas for *GM*=1.26 m.

With increasing *GM*, the natural roll period decreases and the lines corresponding to the resonance move towards the origin *T*=0. Therefore, synchronous rolling becomes more likely while principal parametric resonance will correspond to increasingly shorter waves. Comparing the results for *GM*=0.88 (Figure 4) and 1.26 (Figure 5) m, we see that principal parametric rolling in head waves becomes important for the latter case, especially for low speeds. As in the previous case, principal parametric resonance in following waves can occur only at low speeds, and moves towards stern-quartering waves for larger speeds. The blue dashed line corresponds to the condition T_e=T_φ for the largest ship speed. Synchronous rolling does not seem critical for this case.

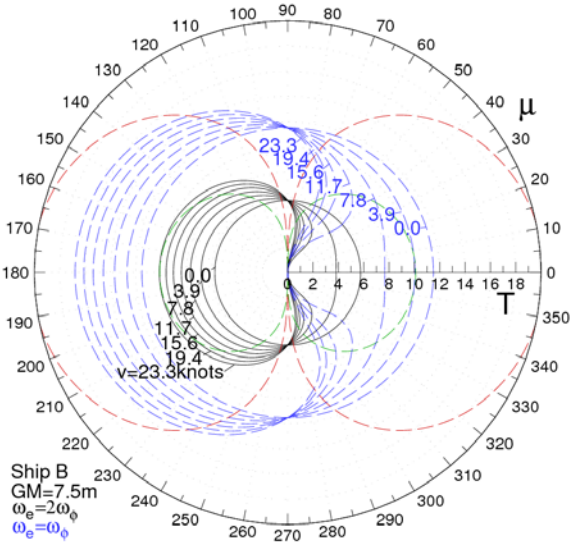

Figure 6. Critical areas for *GM*=7.5 m.

For *GM*=3.797 m (Figure 1), principal parametric resonance in head waves becomes less critical as the resonance lines approach the lower boundary of the suitable wave lengths for small speeds; for larger speeds, parametric rolling in bow waves is usually less critical anyway. Principal parametric resonance in stern-quartering waves corresponds to rather short waves, while synchronous rolling in beam waves corresponds to wave periods of about 18 s, therefore both are unlikely to be important. However, fundamental parametric resonance

can occur in following (for low speeds) or stern-quartering (for higher speeds) waves.

The case with *GM*=7.5 m (see Figure 6) was considered as an example of an extremely high *GM*. For this load case, principal parametric resonance is unlikely as the corresponding waves are too short. On the other hand, synchronous rolling condition corresponds to beam waves with periods of about 13 s, thus becoming important.

5. VERIFICATION

These simple considerations were compared with the results of numerical simulations with *rolls*, shown in Figure 7 as polar colour maps of roll amplitude in axes wave period T – wave direction μ. The plots also show the lines corresponding to resonance conditions $T_e = T_\varphi / 2$ and T_φ with black and blue lines, respectively, as well as the lower and upper boundaries of the area of suitable wave lengths (4) (green and red lines). Each figure shows three polar plots, corresponding to the speeds of 1/3, 2/3 and full design speed (increasing from the left to the right; Froude numbers are indicated).

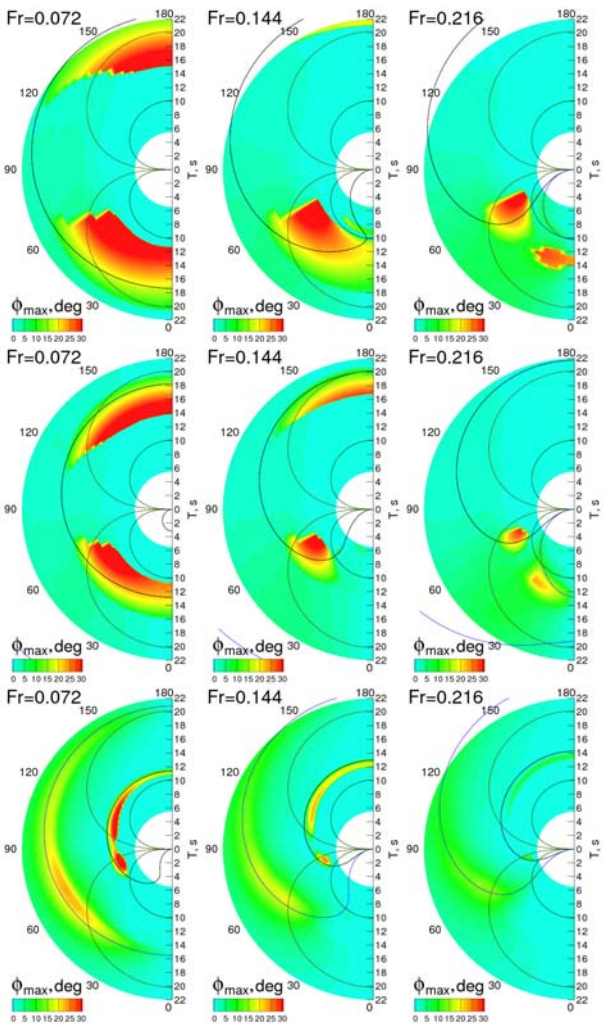

Figure 7. Roll amplitude in regular waves for *GM*=0.88 (top), 1.26, and 3.8 (bottom) m.

The maximum wave period-boundaries of the principal parametric resonance areas follow the resonance line $T_e = T_\varphi / 2$, because they correspond to the onset of parametric rolling with small amplitudes. Roll amplitudes increase in shorter waves for all of the considered load cases, because the natural roll frequency increases with the roll amplitude for this ship. The condition of the suitable wave length (4) bounds the areas of parametric resonance rather well, although they may be broader or narrower than the boundaries (4), depending on wave height and forward speed (hence roll damping).

For *GM*=3.8 m, the area of principal parametric excitation follows the line $\omega_e = 2\omega_\varphi$ even in beam waves for lower speeds. The reason is the variation of righting levers due to large relative heave motions, a phenomenon first discussed by Froude (1861) and studied more recently for a large passenger ship by Ikeda et al. (2005) and Munif et al. (2006). This type of parametric rolling occurs when the ratio of the natural heave and roll frequencies is close to 2 to 1 (here 1.8), and the ship is excited close to the natural heave period in beam waves. Note that time histories of roll motion in such cases show the 2:1 ratio of the roll period to the wave encounter period, characteristic for principal parametric resonance.

Fundamental parametric resonance was also identified, e.g. *Fr*=0.216 for *GM*=0.88 and 1.26 m. The corresponding critical areas are small compared to the areas of principal parametric resonance and synchronous rolling; it is however important that the corresponding roll amplitudes

are large despite high ship speed.

Comparison with the experiments carried out at MARIN for *GM*=0.88, 1.95 and 7.5 m confirms the existence and location of the critical areas. Especially interesting are the results in stern-quartering waves (see an example for *GM*=0.88 m, μ=310° in Figure 8): numerical simulations and model tests show the possibility of principal parametric resonance for oblique wave directions up to 65º off stern. Very close behaviour is obtained in simulations with suppressed yaw motions, indicating that the reason of the excessive roll in these cases is principal parametric excitation. Both experimental and computed time series show that the roll period is double of the encounter wave period, and no synchronous component is visible in the roll response when roll motion grows large enough.

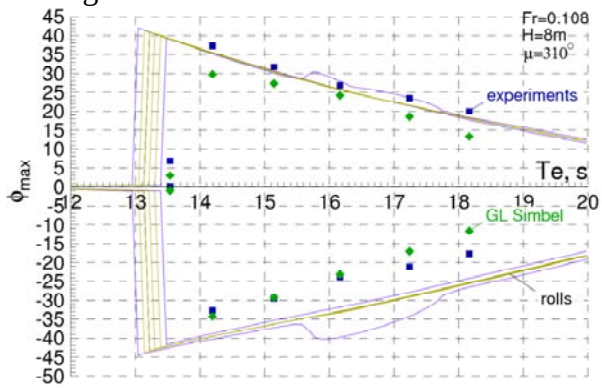

Figure 8. Principal parametric resonance in stern-quartering waves for ship B, *GM*=0.88 m: roll amplitude (positive to starboard, negative to port) vs. wave encounter period

6. IRREGULAR WAVES

Results of numerical simulations in irregular waves also confirm the existence and location of the critical areas. Colour maps of 8 hour-maximum roll angle as function of the wave direction μ and mean wave period T_1 are shown in Figure 9 for ship B with *GM*=0.88 (top) and 1.95 (bottom) m for several ship speeds (increasing from the left to the right). The simulations were carried out in long-crested irregular waves with JONSWAP spectrum with γ=3.3 and significant wave height 8.0 m. In bow and, to a larger degree, in following and stern-quartering waves, the area of large roll responses is stretched in radial direction compared to the responses in regular waves. This is due to the finite breadth of spectrum in irregular waves: the high-frequency tail of the spectrum has sufficient energy to excite parametric or synchronous rolling even if the peak period is large.

Another factor in irregular waves is the dependency of the encounter wave spectrum on the ship speed and wave direction because of the Doppler effect: in a following seaway, the encounter spectrum is narrower than the wave spectrum, which can result in a concentration of wave energy within a narrow range of encounter frequencies for certain ship speeds and wave directions, and thus to stronger excitation. As a simple criterion for this concentration, consider the derivative $d\omega_e/d\omega$, calculated at the peak frequency of the spectrum (equal zero along the lines marked 'c' in Figure 9): when this derivative is small, a larger part of seaway spectrum energy contributes to the excitation around the corresponding encounter frequency. Amplification of roll motion can be seen, especially where this line intersects the

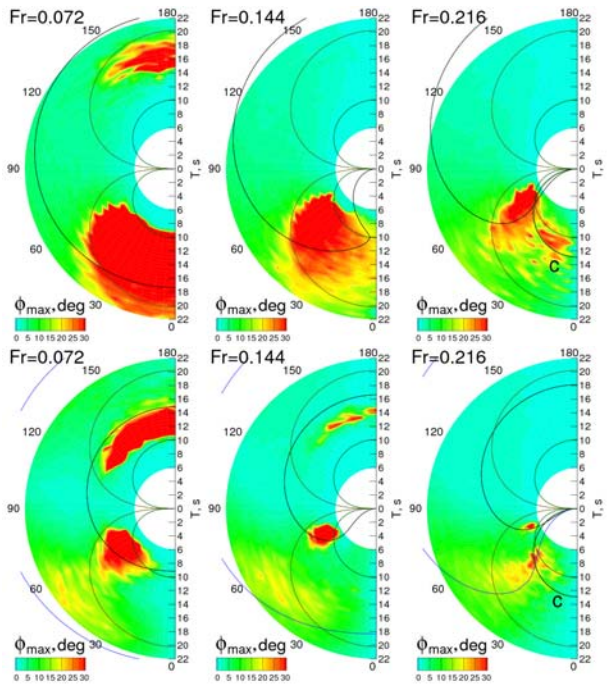

Figure 9. Critical areas in irregular waves for *GM*=0.88 (top) and 1.95 (bottom) m.

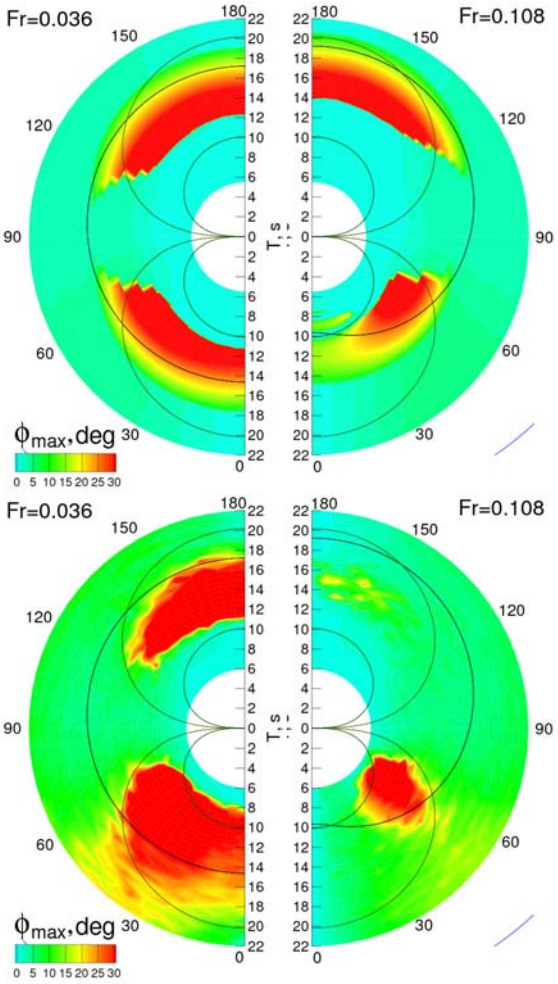

Figure 10. Roll amplitude in regular waves and maximum roll angle in irregular long-crested waves vs. (mean) wave period and (mean) wave direction for ship B, *GM*=1.26 m.

resonance line $T_e = T_\varphi$ for *GM*=1.95 m, *Fr*= 0.216. For $Fr < 0.144$, the waves corresponding to the spectrum concentration condition are (for this ship) too short to be relevant.

In bow waves, the width of the encounter spectrum increases with increasing forward speed. It is well known that the intensity of parametric roll decreases with increasing forward speed in bow waves, see e.g. France et al. (2003), Hashimoto et al. (2007). One of the reasons is increasing roll damping, but it cannot explain the fact that this increase is much stronger in irregular waves than in regular, see also discussions in Francescutto & Bulian (2002) and Belenky (2006). This is illustrated in Figure 10, showing roll amplitude (in regular waves) or 8 hour-maximum roll amplitude (in irregular waves) vs. wave direction and (mean) wave period (circumferential and radial coordinates, respectively). The two top plots show results for *Fr*=0.036 and 0.108 in regular waves, the two bottom ones the corresponding results in irregular waves. In regular waves, increasing Froude number shifts the critical areas due to Doppler effect, with an insignificant decrease of roll amplitudes due to the increased roll damping. In irregular waves, this shift happens together with a large reduction of roll response in bow waves. As roll damping is the same, the reason for this difference should be the widening of encounter spectrum with increasing forward speed in irregular waves: $\mathrm{d}\omega_\mathrm{e} / \mathrm{d}\omega = 1 + 2\omega v g$ (in head waves) increases with increasing forward speed.

In practice, this effect is amplified due to the increase of the added resistance with growing roll amplitudes (France et al., 2003): voluntary speed reduction in a heavy seaway, or a speed drop due to encountering with a high wave, sudden roll etc., leads the ship into a zone of larger roll motions, which in turn reduce the speed even more.

This means that ship designers can select different ways for reducing the danger of parametric rolling:

- select main dimensions and *GM*s in a way avoiding critical responses in frequent seaways,
- design hull form in a way reducing righting arm variations due to waves and vertical motions, see e.g. a study of the influence of geometry variations on parametric roll in Levadou & van't Veer (2006).
- increase roll damping, e.g. using anti-rolling devices,
- or design ship that can maintain high speed in heavy seas, e.g. reducing its susceptibility to slamming and large vertical accelerations.

This also means that the estimation of maximum speed in waves is important for the assessment of dynamic stability.

7. INFLUENCE OF *GM* AND SPEED IN IRREGULAR WAVES

The average (i.e. 'long-term') exceedance rate of maximum lateral acceleration 0.5*g* was calculated for ship C as

$$\bar{r}(LC,v) = \int_{\mu}\int_{T_1}\int_{h_s} r \cdot f \, \mathrm{d}h_s \mathrm{d}T_1 \mathrm{d}\mu \,, \qquad (5)$$

where $r(\mu, T_1, h_s; LC, v)$ is the short-term exceedance rate, depending on the relative wave direction μ, mean seaway period T_1, significant wave height h_s, load case *LC* and forward speed *v* (assumed constant), and $f(\mu, T_1, h_s)$ is the probability density function of seaways for North Atlantic, calculated using the long-term statistics from Söding (2001). r was found from numerical simulations in irregular waves according to the methodology presented in the accompanying paper. Probability density function of wave encounter directions was assumed uniform. A summary of results for three load cases and five forward speeds is shown in Table 1, including contributions from different phenomena to $\bar{r}$: principal parametric resonance (separately for bow waves B, following waves F and oblique-stern waves OS), fundamental resonance in stern waves and synchronous rolling, and average exceedance rate $\bar{r}$ per year for a given load case and ship speed.

Table 1. Results of the calculation of the average exceedance rate.

GM, m	*Fr*	contributions to $\bar{r}$ in %					av. exc. rate per year
		principal resonance			fund., stern	sync.	
		B	OS	F			
0.97	0.00	52.7	20.0	28.3	0.0	0.0	$2.2\cdot10^{4}$
	0.06	21.7	30.0	48.4	0.0	0.0	$1.3\cdot10^{4}$
	0.11	18.3	42.3	39.4	0.0	0.0	$2.0\cdot10^{3}$
	0.17	3.9	25.0	0.0	71.1	0.0	57.0
	0.23	0.1	1.5	0.0	98.4	0.0	$1.9\cdot10^{2}$
2.28	0.00	43.6	28.5	0.7	3.6	23.6	$1.2\cdot10^{2}$
	0.06	91.5	1.0	0.0	0.6	6.9	$1.1\cdot10^{2}$
	0.11	1.3	0.1	0.0	98.6	0.0	2.9
	0.17	0.3	0.0	0.0	99.8	0.0	0.11
	0.23	0.1	0.0	0.0	99.9	0.0	$1.9\cdot10^{-3}$
4.66	0.00	0.0	0.0	0.0	0.0	100	$5.2\cdot10^{2}$
	0.06	0.0	0.0	0.0	0.0	100	$1.2\cdot10^{2}$
	0.11	0.0	0.0	0.0	0.0	100	37.9
	0.17	0.1	0.0	0.0	0.0	99.9	3.0
	0.23	0.0	0.0	0.0	0.0	100	$5.5\cdot10^{-2}$

The relative importance of different dynamic stability problems agrees with the positions of critical areas for different *GM*s and forward speeds:

- For low *GM* and low speed, principal parametric resonance is important both in bow and stern waves. With increasing speed, the contribution of bow directions decreases, while for stern directions, principal parametric resonance moves from following to stern-quartering waves. Further increase of speed increases the contribution from fundamental resonance in stern waves.
- For mean *GM*, principal parametric resonance in following waves is not relevant, while it can occur in oblique-stern waves at small speeds. Important is principal parametric resonance in bow waves (for lower speeds) and fundamental resonance in stern waves for larger speeds.
- For the largest *GM*, synchronous rolling is almost alone relevant for all speeds.

Figure 11 shows the average annual exceedance rate $\bar{r}$ vs. Froude number for the three load cases. The exceedance rate is high at smaller speeds and decreases with increasing forward speed; an exception is the increase between Froude numbers 0.17 and 0.23 for *GM*=0.97 m because of fundamental resonance in stern waves: at smaller forward speeds, the waves required for fundamental resonance are much too long to be relevant.

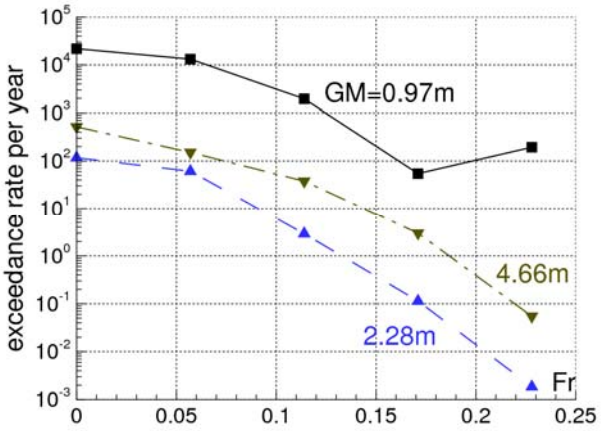

- Figure 11. verage exceedance rate per year of maximum lateral acceleration 0.5*g* vs. Froude number for the three load cases.

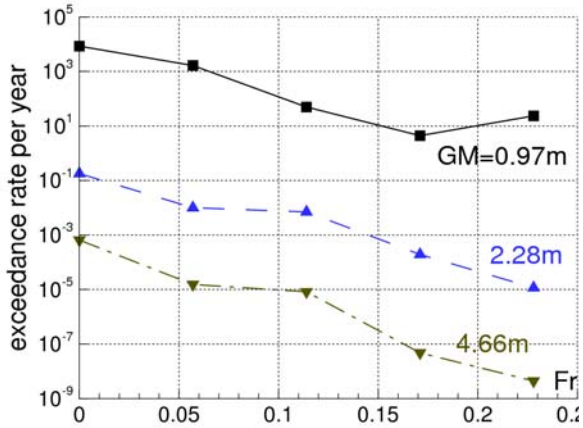

- Figure 12. Average exceedance rate per year of roll angle 40º vs. Froude number.

Another series of simulations was carried out in order to calculate the average exceedance rate of roll angle 40º, which means larger damages and can be used as a criterion for severe accidents. The resulting average exceedance rate per year is shown in Figure 12 vs. Froude number for each load case.

The results for the exceedance rate of 40º roll angle were compared with the results of route simulations of van Daalen et al. (2006), concerning a smaller, 364 TEU container ship. To do this, the calculated average exceedance rates for ship C for different load cases and forward speeds were summed according to the loading and speed profile similar to those used in van Daalen et al. (2006).

The resulting average exceedance rate for ship C is 5.6 per year, or $6.4 \cdot 10^{-4}$ per hour, corresponding to the average hourly exceedance probability of 0.064%. This means that ship C is significantly safer than the ship in van Daalen et al. (2006), for which the average half-hourly capsize probability is 1.4%, which corresponds to the average capsize rate 0.028 per hour or 245.3 per year. This is probably due to the difference in ship sizes.

8. CONCLUSIONS

In the paper, the well-known resonance conditions (1)-(3) are combined with the new form (4) of the wave length condition suitable also for oblique waves, in order to study the location of the areas of excessive roll motions under varying *GM* and forward speed. In irregular waves, an additional factor is the broadening or concentration of the encounter wave spectrum with changing forward speed, which can be quantified by the derivative $\mathrm{d}\omega_\mathrm{e}/\mathrm{d}\omega$, calculated at the peak frequency; for example, an important situation is when this derivative equals zero in stern waves.

The form of polar diagrams ($T-\mu$ axes for constant forward speed) used in the paper is found more convenient than the traditional form ($v-\mu$ axes for constant seaway periods) for the study of the conditions of excessive rolling: the resonance conditions (1)-(3), the wave length condition (4), as well as the spectrum concentration condition $\mathrm{d}\omega_\mathrm{e}/\mathrm{d}\omega|_{\omega_\mathrm{p}}=0$, are all related to wave period. Besides, increased or decreased stiffness of the *GM* curve leads on such diagrams to easily predictable shifts of the critical areas in the radial direction. Finally, this form is more compact: in order to cover the whole parametric space, 4-5 polar plots are required for different ship speeds instead of 10-12 plots for different wave periods.

For other applications, other forms of polar diagrams might be more convenient, e.g. $v-\mu$ diagrams are often considered convenient for operational guidance (Levadou & Gaillarde, 2003, Rathje, 2004, Belenky et al., 2006).

The influence of the location of the critical areas is also studied in irregular waves on the average exceedance rate and on the contributions from different dynamic stability problems. The calculated average exceedance rates illustrate the importance of the ship master actions, and thus of the ship-specific operational guidance assisting the master.

The obtained results also show that the following issues are important in the assessment of the roll motions of a ship: first, further development and validation of the numerical tools, regarding their accuracy in the prediction

of excessive motions and accelerations, particularly in irregular waves. Because of the strong dependency of roll motion on the forward speed, accurate prediction of speed in waves becomes an important problem for stability. This should take into account involuntary speed loss due to the increased resistance in waves, as well as voluntary speed reduction, and result in probability density function of forward speed vs. wave height, direction and period. The same relates to the prediction of viscous roll damping, which should take into account the influence of forward speed and roll damping devices.

9. REFERENCES

Ahmed, T.M., Hudson, D.A., Temarel, P. and Ballard, E.J. (2006) Prediction of parametric roll resonance in longitudinal regular waves using a non-linear method, Proc. STAB 2006, pp. 89-97

Belenky, V.L., Weems, K.M., Lin, W.M. and Paulling, J.R. (2003) Probabilistic analysis of roll parametric resonance in head seas, Proc. STAB 2003, pp. 325-340

Belenky, V., Yu, H.-C. and Weems, K. (2006) Numerical procedures and practical experience of assessment of parametric roll of container carriers, Proc. STAB 2006, pp. 119-130

Blume, P. (1976) Zur Frage der erregenden Längskraft in von achtern kommenden regelmäßigen Wellen. Report No.334, Institut für Schiffbau, Hamburg

Blume, P. (1979) Experimentelle Bestimmung von Koeffizienten der wirksamen Rolldämpfung und ihre Anwendung zur Abschätzung extremer Rollwinkel, Schiffstechnik 25(1) 3-29

Böttcher, H. (1986) Ship motion simulation in a seaway using detailed hydrodynamic force coefficients, Proc. STAB'86

Brunswig, J., Pereira, R. and Kim, D.-W. (2006) Validation of parametric roll motion predictions for a modern containership design, Proc. STAB 2006

Bulian, G., Francescutto, A. and Lugni, C. (2003) On the nonlinear modelling of parametric rolling in regular and irregular waves, Proc. STAB 2003, pp. 305-323

Bulian, G., Lugni, C. and Francescutto, A. (2004) A contribution on the problem of practical ergodicity of parametric roll in longitudinal long-crested irregular sea, Proc., 7th Int. Ship Stability Workshop

van Daalen, E.F.G., Boonstra, H. and Blok, J.J. (2006) Capsize probability analysis for a small container vessel, IMO, SLF 49/INF.7

DeKat, J. O. and Paulling, J. R. (1989) The simulation of ship motions and capsizing in severe seas, SNAME Transactions 97, pp. 139-168

France, W.N., Levadou, M., Treakle, T.W., Paulling, J.R., Michel, R.K. and Moore, C. (2003) An investigation of head-sea parametric rolling and its influence on container lashing systems, Marine Technology 40, pp. 1-19

Francescutto, A. and Bulian, G. (2002) Nonlinear and stochastic aspects of parametric rolling modelling, Proc., Int. Ship Stability Workshop, Webb Inst.

Froude, W. (1861) On the rolling of ships. In: The Papers of William Froude. – RINA, London 1955

Graff, W. and Heckscher, E. (1941) Widerstands- und Stabilitäts-Versuche mit drei Fischdampfermodellen, Werft-Reederei-Hafen 22, pp. 115-120

Grim, O. (1961) Beitrag zu dem Problem der Sicherheit des Schiffes im Seegang, Schiff und Hafen 490

Hashimoto, H., Umeda, N. Matsuda, A. and Nakamura, S. (2006) Experimental and numerical studies on parametric roll of a post-panamax container ship in irregular waves, Proc. STAB 2006, pp. 181-190

Hashimoto, H., Umeda, N. and Sakamoto, G. (2007) Head-sea parametric rolling of a car carrier, Proc. 9th Int. Ship Stability Workshop, pp. 451-457

Hennig, J., Billerbeck, H., Clauss, G., Testa, D., Brink, K.-E. and Kühnlein, W.L. (2006) Qualitative and quantitative validation of a numerical code for the realistic simulation of various ship motion scenarios, Proc. OMAE 2006

Hua, J., Palmquist, M. and Lindgren, G. (2006) An analysis of the parametric roll events measured onboard the PCTC Aida, Proc. STAB 2003, pp. 109-118

Ikeda, Y., Munif, A., Katayama, T. and Fujiwara, T. (2005) Large parametric rolling of a large passenger ship in beam seas and role of bilge keels in its restraint, Proc. 8th Int. Ship Stability Workshop

Kempf, G. (1938) Die Stabilitätsbeanspruchung der Schiffe durch Wellen und Schwingungen, Werft-Reederei-Hafen 19, pp. 200-202

Kerwin, J. E. (1955) Note on rolling in longitudinal waves, Int. Shipbuilding Progress 2(16) pp. 597-614

Kröger, P. (1987) Roll Simulation von Schiffen im Seegang, Schiffstechnik 33, pp. 187-216

Krüger, S. and Kluwe, F. (2006) Development of dynamic stability criteria from direct seakeeping simulations, Proc. 9th Int. Marine Design Conf.

Levadou, M. and Gaillarde, G. (2003) Operational guidance to avoid parametric roll, Proc. Conf. Design and Operation of Container Ships, pp. 75-86

Levadou, M. and van't Veer, R. (2006) Parametric roll and ship design, Proc. STAB 2006, pp. 191-206

Munif, A., Ikeda, Y., Fujiwara, T. and Katayama, T. (2006) Parametric roll resonance of a large passenger ship in dead ship condition in all heading angles, Proc. STAB 2006, pp. 81-87

MSC/Circ.707 (1995) Guidance to the master for avoiding dangerous situations in following and quartering seas

Neves, M.A.S. and Rodríguez, C.A. (2006) An investigation on roll parametric resonance in regular waves, Proc. STAB 2006, pp. 99-108

Paulling, J. R. (1961) The transverse stability of a ship in a longitudinal seaway, J. Ship Research 4(4) pp. 37-49

Pereira, R. (1988) Simulation nichtlinearer Seegangslasten, Schiffstechnik 35, pp. 173-193

Petey, F. (1986) Forces and moments due to fluid motions in tanks and damaged compartments, Proc. STAB'86

Rathje, H. (2004) Shipboard routing assistance, Schiff und Hafen 11

Salui, K. B., Shigunov, V. and Vassalos, D. (2004) A RANS based method for the estimation of ship roll damping with forward speed, Proc. OMAE 2004

SLF 50/INF.2 (2007) Proposal on additional intact stability regulations, submitted by Germany

SLF 51/INF.3 (2008) New generation intact stability criteria, submitted by Germany

Söding, H. (1982) Leckstabilität im Seegang. Rep. 429, Institut für Schiffbau, Hamburg

Söding, H. (2001) Global seaway statistics, Schiffstechnik 48, pp. 147-153

Spanos, D. and Papanikolaou, A. (2006) Numerical simulation of parametric roll in head seas, Proc. STAB 2006, pp. 169-180

Umeda, N., Hashimoto, H., Vassalos, D., Urano, S. and Okohu, K. (2003) Nonlinear dynamics of parametric roll resonance with realistic numerical modelling, Proc. STAB 2003, pp. 281-290